

# Preparation of Rhodium Catalysts Supported on Carbon Nanotubes by a Surface Mediated Organometallic Reaction

Roberto Giordano,<sup>[a]</sup> Philippe Serp,<sup>\*[a]</sup> Philippe Kalck,<sup>[a]</sup> Yolande Kihn,<sup>[b]</sup>  
Joachim Schreiber,<sup>[c]</sup> Christiane Marhic,<sup>[c]</sup> and Jean-Luc Duvail<sup>[c]</sup>

**Keywords:** Nanotubes / Rhodium / Supported catalysts / Surface chemistry / Heterogeneous catalysis

The dimeric complex  $[\text{Rh}_2\text{Cl}_2(\text{CO})_4]$  was grafted to multi-walled carbon nanotubes (MWNTs) previously oxidised with nitric acid and then treated with sodium carbonate to produce carboxylate groups on their outer surface. The grafting mechanism involves bridge-splitting and substitution of -COO for Cl, as evidenced by the presence of NaCl in the samples. A further reduction/decomposition step under dihydrogen at 573 K afforded highly dispersed rhodium nanoparticles ( $\approx 1.5\text{--}2.5$  nm). This novel rhodium-supported carbon material (Rh/MWNT-COONa) was tested as a catalyst for the hydrogenation of *trans*-cinnamaldehyde and the hydroformylation of hex-1-ene in the liquid phase: in both cases it was found to be very selective, toward C=C double-bond hy-

drogenation and the production of linear and branched aldehydes, respectively. A comparison was made between its catalytic activity and that of rhodium supported on pristine MWNTs and on nitric acid-oxidised MWNTs. We observed that these latter catalysts have larger particle sizes and lower activities, thus confirming the efficiency of our grafting procedure. Moreover, the better results obtained when using MWNT-COONa as support with respect to carboxylate-containing activated carbon also point to the important role played by the mesoporous nature of the carbon nanotube support, which can ameliorate transfer processes.  
(© Wiley-VCH Verlag GmbH & Co. KGaA, 69451 Weinheim, Germany, 2003)

## Introduction

Carbon materials are attractive supports in heterogeneous catalytic processes owing to their ability to be tailored to meet specific needs. Indeed, activated forms of carbon are currently employed as catalyst supports because of their high surface area, their stability at high temperatures under a nonoxidising atmosphere and the possibility of controlling both their porous structure and the chemical nature of their surface.<sup>[1,2]</sup> New forms of carbon have appeared during the last decade, showing novel interesting potentialities as supports.<sup>[3]</sup> Carbon nanofibres, also called graphite nanofibres, and carbon nanotubes, have so far been used successfully and shown to present, as final supported materials, catalytic properties superior to those of catalysts prepared on activated carbon, soot, or graphite.<sup>[2]</sup> Whilst carbon nanofibres consist of graphite sheets arranged in various ori-

entations along the fibre axis — the most common structure being the one in which the planes are stacked up like a fishbone, with a lot of edges — both single-walled (SWNT)- and multi-walled (MWNT) carbon nanotubes show a concentric wall structure consisting of ordered graphite platelets. The morphology and the size of the above supports, especially since they present huge lengths vs. diameters, can play a significant role in catalytic applications owing to their ability to disperse the active phase. Their electronic properties are also of primary importance,<sup>[4]</sup> and their mechanical strength makes them resistant in view of recycling. A recent comparison between the interaction of transition metal atoms with carbon nanotube walls and with graphite indicates major differences in bonding sites, magnetic moments and charge-transfer direction.<sup>[5]</sup>

The most widely used technique to achieve the deposition of metals on the above materials is the incipient wetness impregnation one, in which the purified carrier is impregnated with a solution of the metal precursor, then dried, calcinated and/or reduced so as to obtain metal particles dispersed on the support.<sup>[3,6]</sup> Several studies have been performed on graphite-nanofibre-supported Fe-Cu,<sup>[7]</sup> Ni<sup>[8]</sup> or Pd<sup>[9]</sup> particles for catalytic hydrogenation. Graphite-nanofibre-supported rhodium catalysts were found to be active in ethene hydroformylation.<sup>[10]</sup> If we consider the use of carbon nanotubes, several examples are worth mentioning: Cu

<sup>[a]</sup> Laboratoire de Catalyse, Chimie Fine et Polymères, Ecole Nationale Supérieure des Ingénieurs en Arts Chimiques Et Technologiques, 118 route de Narbonne, 31077 Toulouse Cédex 4, France  
Fax: (internat.) +33-5/6288-5600  
E-mail: philippe.serp@ensiacet.fr

<sup>[b]</sup> CEMES-CNRS no. 8011, 2 rue Jeanne Marvig, 31055 Toulouse, France

<sup>[c]</sup> Institut des Matériaux Jean Rouxel-UMR 6502, Université de Nantes, 2 rue de le Houssinière, BP 32229, 44322 Nantes Cédex 3, France

nanoparticles were synthesised employing SWNTs as a template;<sup>[11]</sup> Ru/SWNTs<sup>[12]</sup> and alkali-promoted Ru/MWNTs<sup>[13]</sup> catalysts were prepared for hydrogenation reactions and for ammonia synthesis, respectively; Pd, Pt, Ag and Au nanoparticles were grown on SWNTs, and their size could be adjusted by changing the metal to carbon ratio;<sup>[14]</sup> Rh/MWNTs catalysts for propene hydroformylation were prepared by incipient wetness impregnation from benzene solutions of  $[\text{RhH}(\text{CO})(\text{PPh}_3)_3]$  on pristine nanotubes.<sup>[15]</sup>

Chemical treatment and/or modification of the surface of carbon nanotubes was found to be a useful tool for controlling their hydrophobic or hydrophilic character,<sup>[16]</sup> and studies carried out in order to accomplish the deposition of metals point to a strong interaction between metal atoms and the groups created by oxidation of the support surface.<sup>[17]</sup>

Thus, graphite nanofibre-supported iron Fischer–Tropsch catalysts have been prepared by three different methods on  $\text{HNO}_3$ -treated supports.<sup>[18]</sup> Important improvements toward the preparation of selective hydrogenation catalysts were achieved by supporting Pt on SWNTs oxidised in dilute  $\text{HNO}_3$ ; the bonding between platinum and the carbon nanotube surface was presumably accomplished by ion-exchange on the carboxylic acid sites so formed.<sup>[19]</sup> Another example of such reactivity is the replacement of the proton of carboxylic groups with uranyl ions: XPS studies of oxidised nanotubes revealed that their surface is covered by carboxylic, carbonyl and hydroxyl groups, and, in particular, the presence of  $-\text{COOH}$  groups could be used to initiate nucleation on the support surface, leading to the selective covering of the outer surface by metallic species.<sup>[20]</sup> A Co/MWNTs system showing a good catalytic activity in dehydrogenation was prepared by oxidising MWNTs in boiling nitric acid prior to impregnation with a cobalt salt, followed by drying, calcination and reduction with  $\text{H}_2$ .<sup>[21]</sup>

Bimetallic Ru/Pt and Ru/Sn nanoparticles have been prepared from molecular heterobimetallic carbonyl clusters deposited on MWNTs previously treated with  $\text{HNO}_3$ .<sup>[22]</sup> A heterobimetallic precursor was also used to prepare Pt–Ru anode catalysts supported on oxidised and nonoxidised carbon nanofibres, SWNTs and MWNTs.<sup>[23]</sup> Coordination of Pd on  $\text{HNO}_3$ -treated carbon nanofibres<sup>[24]</sup> and of Pt on  $\text{H}_2\text{SO}_4/\text{HNO}_3$ -treated MWNTs has also been reported.<sup>[25]</sup>

A suitable technique to achieve the grafting of metal particles onto carbon nanotubes would therefore consist of functionalising the outer surface of the tubes and then performing a chemical reaction with a metal complex. This was initially accomplished by reacting Vaska's complex  $[\text{IrCl}(\text{CO})(\text{PPh}_3)_2]$  with a  $\text{HNO}_3$ -oxidised support: the tethering reaction occurs by coordination of iridium to the nanotubes through the oxygen atoms.<sup>[26]</sup>

Furthermore, a controlled chemical grafting of a metal species to the surface of carbon nanotubes would very likely result in a fine dispersion of metallic particles.

In this paper we describe a new technique that involves the organometallic reaction of the rhodium complex  $[\text{Rh}_2\text{Cl}_2(\text{CO})_4]$  with a modified MWNT surface bearing sodium carboxylate groups, which permits the production of

highly dispersed Rh nanoparticles, after a decomposition/reduction step. We also report some preliminary results concerning the catalytic activity of these novel materials either in hydrogenation or hydroformylation reactions. Last but not least, the catalytic activity of these materials is compared to that observed when using rhodium-supported catalysts prepared by reacting  $[\text{Rh}_2\text{Cl}_2(\text{CO})_4]$  with pristine or  $\text{HNO}_3$ -treated MWNTs, as well as with activated carbon bearing sodium carboxylate groups.

## Results and Discussion

### Surface Modification of MWNTs

High purity samples of MWNTs were employed for this study (MWNTs 97%, the remaining 3% coming from iron nanoparticles encapsulated within the nanotubes and generated by the catalytic production process).<sup>[27]</sup> Typical TEM micrographs of this material are shown in Figure 1.

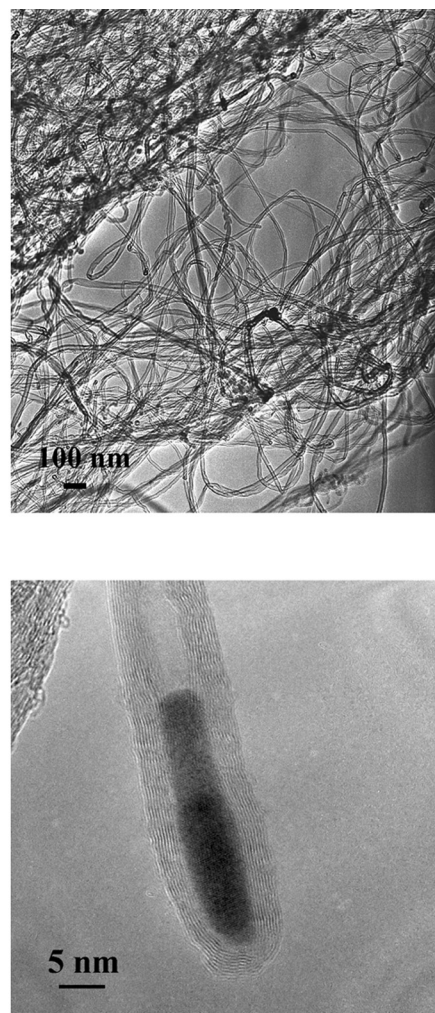
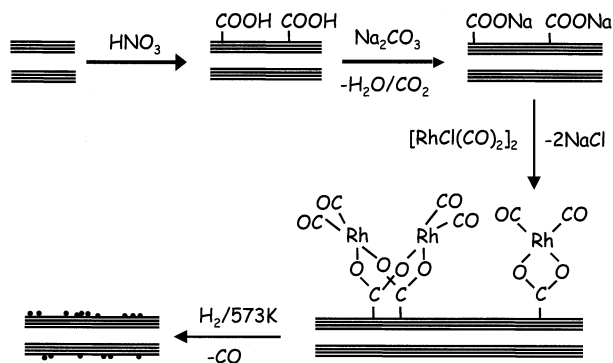


Figure 1. Typical TEM micrographs of pristine MWNTs

It consists of graphene layers (interlayer spacing  $d_{002} = 0.342$  nm) arranged in a roughly parallel way with respect to the tube axis. Mean tube external and internal diameters

are 17 nm and 8 nm, respectively, which corresponds to about 13 walls. These nanotubes are characterised by a length of several micrometers and a specific surface area of about  $180 \text{ m}^2 \cdot \text{g}^{-1}$ , with no microporosity. Pores in aggregated MWNTs can be mainly divided into inner hollow cavities of small diameter (3–9 nm) and aggregated pores (15–25 nm) formed by interaction of isolated MWNTs.<sup>[28]</sup> From TEM observations it appears that one end of the tube is closed by graphene layers, the remaining iron carbide nanoparticles being located either at the tip of the tubes (see Figure 1) or in their inner cavities. Moreover, this material is highly hydrophobic since it does not present oxygen-containing groups, and therefore it should be unsuitable for supporting metallic nanoparticles.<sup>[29]</sup>

Thus, we envisaged to investigate the effect of chemical surface modifications on the feasibility of the grafting of the complex  $[\text{Rh}_2\text{Cl}_2(\text{CO})_4]$  and on the subsequent nanoparticle formation process by reductive treatment under  $\text{H}_2$ . Bridge-splitting and replacement reactions of rhodium carbonyl chloride dimer have been known for many years and often involve the use of silver carboxylate salts as reagents.<sup>[30]</sup> As it is well-known that oxidation of carbon nanotubes with nitric acid mainly generates carboxylic groups on the surface,<sup>[17b]</sup> we decided to investigate the possibility of synthesising the corresponding sodium carboxylates and hence of producing a true *nanotube salt*. Therefore the surface-mediated organometallic reaction depicted in Scheme 1 would be expected to occur on treatment with the dirhodium precursor, leading to a molecular dispersion of Rh carbonyl species and to a high dispersion of metallic particles after a further decomposition/reduction step (Scheme 1).



Scheme 1. Surface mediated organometallic reaction between  $[\text{Rh}_2(\mu\text{-Cl})_2(\text{CO})_4]$  and MWNT-COONa

From TEM micrographs it appears that the morphology of MWNT-COOH and MWNT-COONa does not differ significantly from that of pristine tubes. Thus, under our experimental conditions the oxidation treatment performed causes only minor damage to the tips of the nanotubes (Figure 2). Raman spectra recorded either on pristine tubes or on oxidised samples clearly indicate that oxidation does not affect the degree of graphitisation of these materials (Figure 3). In both cases the graphite mode G-band and the defect mode D-band possess nearly the same intensities.

Furthermore, a slight increase in the surface area is observed in the case of MWNT-COOH ( $S_{\text{BET}} = 200 \text{ m}^2 \cdot \text{g}^{-1}$ ).

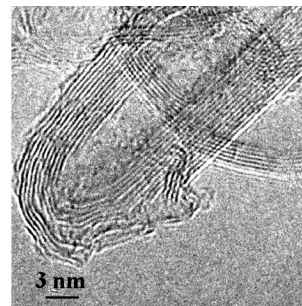


Figure 2. TEM micrograph of  $\text{HNO}_3$ -treated MWNTs

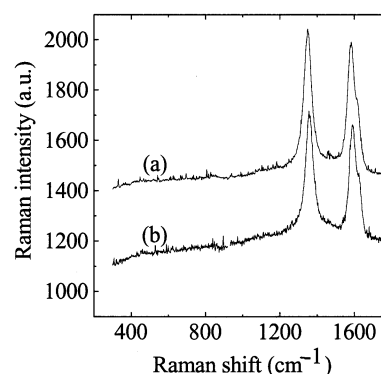


Figure 3. Raman spectra of: (a) pristine MWNTs and (b) MWNT-COOH

In order to examine the carbon environment on the surface, XPS analyses were performed on the different samples; the relevant data are given in Table 1.

Table 1. XPS data obtained from MWNT samples

Sample	Binding Energy <sup>[a]</sup> (eV)				S <sup>[b]</sup>	O <sup>[b]</sup>	C <sup>[b]</sup>	Na <sup>[b]</sup>
	530.9	532.1	533.2	534.2				
MWNT	55	45	—	—	0.14	0.81	99.05	—
MWNT-COOH	23	44	24	9	—	3.23	96.77	—
MWNT-COONa	25	49	—	14	—	5.29	93.04	1.67

<sup>[a]</sup> Values given as % of the total amount. <sup>[b]</sup> Atomic percentage.

The ratio of total oxygen to total carbon is a measure of the degree of surface oxidation, and reconstruction of the O1s peak gives additional information about the surface oxygen-containing groups. XPS spectra of all the modified MWNT samples show an increase of the oxygen content. The MWNT-COOH sample exhibits functionalities that contribute to the intensity of the O1s peaks located at 530.9 eV, 532.1 eV, 533.2 eV and 534.2 eV, in agreement with published data for activated carbon treated with nitric acid.<sup>[31]</sup> Hence, this type of treatment significantly increases

the amount of surface carboxylic groups. As for MWNT-COONa, a new peak appears at 535.4 eV, which can be attributed to the sodium carboxylate groups<sup>[32]</sup> (an XPS analysis performed on a CH<sub>3</sub>COONa sample gave a value of 534.9 eV for -COONa). The presence of sodium was confirmed by the Na1s peak at 1071.5 eV.

The formation of sodium carboxylate groups on the outer surface of MWNTs makes this material highly hydrophilic, and it can easily be dispersed in water. Moreover, it is interesting to note that a small amount (ca. 5 mg·L<sup>-1</sup>) of the so formed MWNT sodium salt is dissolved during washing with water, performed to remove the excess of sodium carbonate.

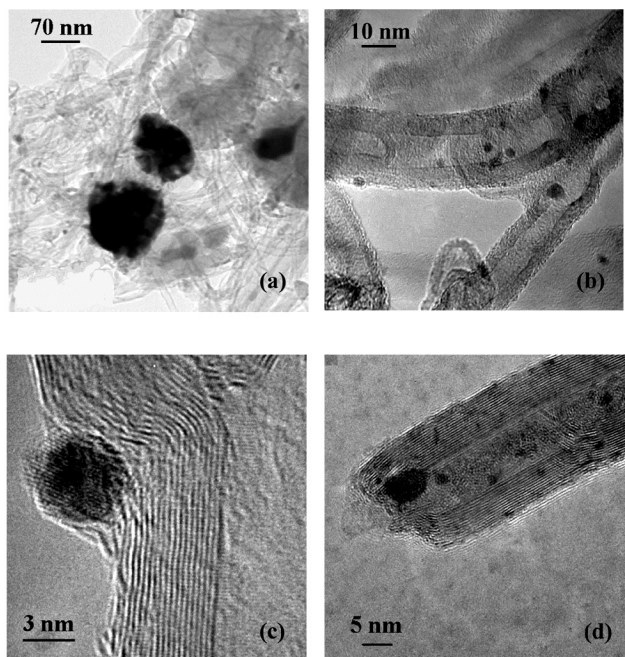


Figure 4. TEM micrographs of: (a) 1%Rh/MWNTs; (b) and (c) 1%Rh/MWNT-COOH; (d) 1%Rh/MWNT-COONa

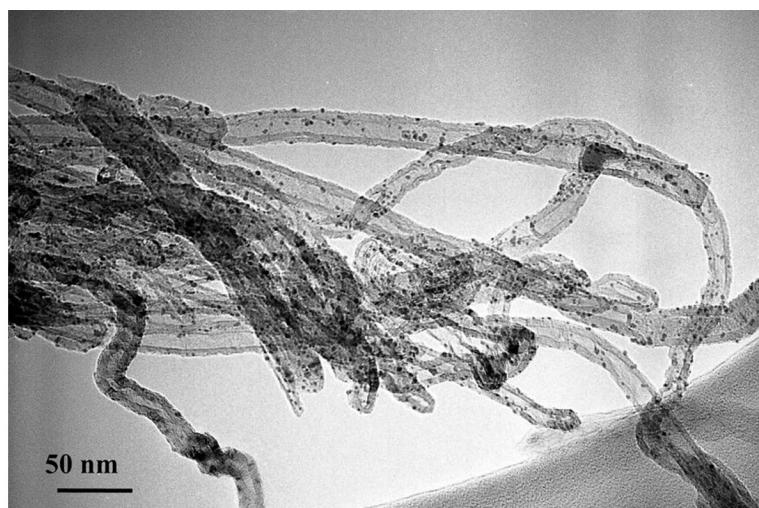


Figure 5. TEM micrographs of 9.5%Rh/MWNT-COONa

### Rh/MWNTs Catalyst Preparation by [Rh<sub>2</sub>Cl<sub>2</sub>(CO)<sub>4</sub>] Grafting

The grafting procedure described above involves the reaction between toluene solutions of [Rh<sub>2</sub>Cl<sub>2</sub>(CO)<sub>4</sub>] and various supports, namely MWNTs, MWNT-COOH, MWNT-COONa and C\*-COONa. It is worth noting that with a loading of Rh equal to 1% w/w, whatever the carbon nanotube support employed, after impregnation and filtration the resulting solution is always colourless, pointing to a complete adsorption of the rhodium complex by some interaction between the complex and the MWNTs. IR spectra of these toluene solutions confirmed the absence of any detectable carbonyl bands due to rhodium species. Moreover, infrared and Raman spectra of all the solid samples obtained via the grafting procedure showed no bands attributable to the carbonyl ligands; this could very likely be due to the low rhodium loading (1–5% w/w), although the possibility of a decarbonylation reaction occurring during the grafting/drying procedure should also be considered. Furthermore, in the case of the reaction between [Rh<sub>2</sub>Cl<sub>2</sub>(CO)<sub>4</sub>] and MWNT-COONa, the observation by X-ray diffraction of the presence of NaCl in the samples coming from decomposition under dihydrogen clearly indicates the occurrence of the carboxylate group mediated grafting of the complex through bridge splitting.

After reductive decomposition at 573 K, careful rinsing with water to remove NaCl, and drying at 383 K under vacuum overnight, all of the samples were examined by TEM (Figure 4 and 5).

In the case of Rh/MWNTs the very large particle size distribution observed (particle size up to 100 nm has been measured) points to a weak interaction between the metal carbonyl precursor and the tube surface, which favours the migration and agglomeration of the rhodium(0) atoms deriving from the decomposition/reduction steps. As for Rh/MWNT-COOH, a better dispersion is obtained (mean particle size 2.5–5 nm), indicating that a reaction has occurred between the -COOH groups and the rhodium complex.

However, the results obtained with MWNT-COONa (mean particle size  $\approx 1.5\text{--}2.5$  nm) clearly show that the grafting to carboxylate groups is more efficient. Indeed, the reaction of surface carboxylate groups with the dirhodium precursor, which gives better results with respect to particle size and dispersion, is expected to be different from that of the carboxylic groups, owing to the higher nucleophilicity of the two oxygen atoms of the anionic  $\text{-COO}^-$  moiety and to the symmetric distribution of the charge (the hydrogen atom having been removed).

The MWNT sodium salt can hence be considered as a primary ligand that would be prone to react with the dirhodiumchlorocarbonyl dimeric complex to produce rhodium species grafted to the surface via splitting of the Cl bridges. Further decomposition under  $\text{H}_2$  affords highly dispersed rhodium-supported particles even with metal loadings up to 9.5% w/w: a mean particle size of 3 nm has been measured in the case of 9.5% Rh/MWNT-COONa, with a very narrow ( $3 \pm 2$  nm) particle size distribution (see Figure 5).

### Catalytic Experiments

In general, we have investigated liquid-phase catalytic reactions in order to determine whether the peculiar structures of MWNTs, and particularly their high mesoporosity, could improve transfer phenomena with respect to highly microporous activated carbons. Additionally, we were interested in the possibility of comparing surface-mediated organometallic synthesis methods to more classical impregnation techniques involving prior oxidation by nitric acid. Two reactions were studied: the hydrogenation of *trans*-cinnamaldehyde and the hydroformylation of hex-1-ene.

Prior to evaluating the catalytic activity of rhodium-supported catalysts, blank experiments were performed with MWNTs and MWNT-COOH in order to check the possible role of the remaining 3% w/w iron nanoparticles, encapsulated within the nanotubes, in the investigated catalytic systems. For MWNTs no activity was observed either in hydrogenation or in hydroformylation; in the case of MWNT-COOH a 1.7% conversion into hydrocinnamaldehyde was obtained, whilst no hydroformylation product could be detected. Indeed, iron nanoparticles of approx.  $5 \times 20$  nm size, located either at the tip, or in inner cavities, of the nanotubes, are not accessible to the reactants in the case of MWNTs owing to the presence of graphene layers roughly perpendicular to the axis of MWNTs (bamboo-like structure), as shown on Figure 6. As depicted in Figure 2, the nitric acid treatment induces opening of the tip of the tubes, thus making iron particles reachable by the reactants. Since iron-based supported catalysts are known to be active in alkene hydrogenation,<sup>[33]</sup> it is very likely that the observed activity could actually be due to the presence of zero-valent iron and/or iron carbide particles.

### Selective Hydrogenation of *trans*-Cinnamaldehyde

The catalytic results of liquid-phase hydrogenation of *trans*-cinnamaldehyde are depicted in Table 2.

One can observe that, except in the case of Rh/MWNTs, all these catalytic systems selectively afford hydrocinnamal-

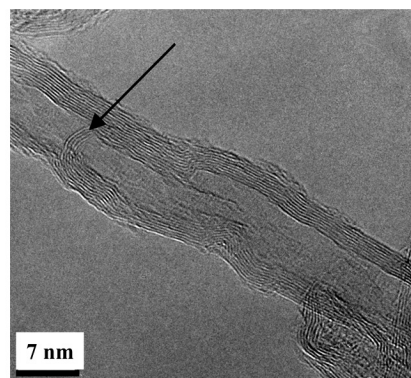


Figure 6. TEM micrograph showing graphene layers closing the inner cavity of a MWNT

Table 2. Catalytic hydrogenation of *trans*-cinnamaldehyde

Catalyst	Conv (%)	Activity <sup>[a]</sup>	Selectivity <sup>[b]</sup>
1% Rh/MWNT	—	—	—
1% Rh/MWNT-COOH	5.3	26.8	100.0
1% Rh/MWNT-COONa	15.1	78.2	100.0
9.5% Rh/MWNT-COONa	23.2	11.4	100.0
1% Rh/C*-COONa	4.9	27.1	100.0
5% Pd/C* <sup>[c]</sup>	62.8	343.3	64.5 <sup>[d]</sup>

<sup>[a]</sup> In g substrate transformed  $\cdot \text{g}^{-1}_{\text{Rh}} \cdot \text{h}^{-1}$   $\text{g}^{-1}_{\text{Rh}} \cdot \text{h}^{-1}$ . <sup>[b]</sup> % cinnamaldehyde. <sup>[c]</sup> A commercial 5% w/w Pd/C\* (Johnson Matthey) was used for comparison purposes. <sup>[d]</sup> Hydrocinnamyl alcohol was the other product of the reaction.

dehyde through C=C double bond hydrogenation, irrespective of the Rh-supported carbon sample employed.

The Rh/MWNTs samples, in accordance with TEM micrographs in which very large rhodium aggregates can be observed, possess no catalytic activity. In contrast, Rh/MWNT-COOH and Rh/MWNT-COONa are active and very selective catalysts for hydrocinnamaldehyde formation. If one compares the selectivity data, Rh-supported catalysts are more selective than a commercial Pd/C\* catalyst, in that C=C double bond hydrogenation is the only reaction occurring under our experimental conditions.

As far as catalytic activity and conversion are concerned, it appears that the best method to support Rh particles on the MWNTs surface is indeed the grafting of the complex via surface-mediated organometallic synthesis, followed by reduction under  $\text{H}_2$ . The good performance of the thus-prepared catalysts can hence be attributed to the very small particle size obtained after the decomposition/reduction step and to the high purity of the metallic deposit. Higher conversion together with lower activity values for a 9.5% loading of rhodium on MWNTs could be attributed to the effect of the larger particle size observed. As for mass-transfer limitations, the complete absence of microporosity, together with a relatively high surface area, are crucial to a good catalytic activity. For instance, if we compare the Rh/MWNT-COONa catalyst to Rh/C\*-COONa prepared ac-

ording to the same procedure, the former is three times more active.

### Hydroformylation of Hex-1-ene

Liquid-phase hydroformylation runs were carried out with hex-1-ene under relatively mild conditions (2 MPa, 353 K) and afforded *n*-heptanal and 2-methylhexanal, together with 2-ethylpentanal. The presence of the last product is due to partial isomerization of the substrate to hex-2-ene, which has been observed in the reaction solutions by GC. Such a reaction pathway was previously observed under more drastic conditions (10 MPa, 423 K) on Rh/C\* catalysts,<sup>[34]</sup> leading to C7 aldehyde, hexane and C7 alcohol formation. The catalytic results are shown in Table 3, and the selectivities to the products obtained are listed in Table 4.

It should be noted that the production of linear and branched aldehydes and a high linear/branched ratio (2.6) occur only with 1% Rh/MWNT-COOH, a sample characterised by large particle sizes and by the acidic character of the support. In this case no ethylpentanal and lower amounts of methylhexanal were detected. The most important feature of our catalytic system is the high conversion and activity values found for 1% Rh/MWNT-COONa and the selectivity of the reaction toward aldehyde formation, thus confirming, as for *trans*-cinnamaldehyde hydrogenation, the efficiency of our grafting method and the advantage

of using carbon nanotubes as a support in liquid-phase catalytic reactions.

### Conclusion

Oxidation of the outer surface of multi-walled carbon nanotubes by nitric acid leads to the formation of carboxylic groups that can be used to anchor rhodium carbonyl moieties. Better results are obtained upon conversion of carboxylic into more reactive carboxylate groups. A further reduction step under dihydrogen affords highly dispersed (for instance 1.5–2.5 nm for a 1% w/w loading) rhodium nanoparticles even for rhodium loadings up to 9.5% w/w. These Rh-supported catalysts show interesting performances with respect to liquid-phase hydrogenation and hydroformylation reactions. Additionally, the nature of the MWNT support probably contributes to a better activity, presumably by ameliorating transfer processes with respect to what happens on classical activated carbons.

### Experimental Section

**General Remarks:** Nitric acid (Prolabo, 52.5%), Na<sub>2</sub>CO<sub>3</sub>·10H<sub>2</sub>O (Acros Organics), toluene (Acros Organics, 99%), dioxane (SDS), *trans*-cinnamaldehyde (Aldrich, 98%) and hex-1-ene (Janssen, 97%) were used as received. H<sub>2</sub> and CO (Air Liquide, 99.99998 and 99.99%, respectively) were also used as received. The complex [Rh<sub>2</sub>Cl<sub>2</sub>(CO)<sub>4</sub>] was prepared according to a well established procedure.<sup>[36]</sup>

Carbon nanotubes were prepared by a catalytic CVD method<sup>[27]</sup> on an Fe/Al<sub>2</sub>O<sub>3</sub> catalyst.<sup>[35]</sup> Dissolution of the alumina support and some of the iron was performed by acidic treatment (H<sub>2</sub>SO<sub>4</sub>, 98% Prolabo). Typical characterisation data for this material are given in Table 5.

#### Surface Modification of MWNTs

A mixture of 5 g of MWNTs in 150 mL of HNO<sub>3</sub> (52.5%) was refluxed for 3 hours at 403 K. Then the mixture was filtered and

Table 3. Catalytic hydroformylation of hex-1-ene

Catalyst	Conv. (%)	Activity <sup>[a]</sup>	n/b ratio <sup>[b]</sup>
1% Rh/MWNT	–	–	–
1% Rh/MWNT-COOH	52.3	72.9	2.6
1% Rh/MWNT-COONa	75.8	197.6	1.2
9.5% Rh/MWNT-COONa	65.8	11.6	1.2
1%Rh/C*-COONa	66.1	105.6	1.2

<sup>[a]</sup> In g substrate transformed·g<sup>-1</sup><sub>Rh</sub>·h<sup>-1</sup> in g<sup>-1</sup><sub>Rh</sub>·h<sup>-1</sup>. <sup>[b]</sup> n = linear isomer; b = branched isomer.

Table 4. Product distribution for hex-1-ene hydroformylation (as selectivities, %)

Catalyst	2-Ethyl-pentanal	2-Methyl-hexanal	Heptanal
1% Rh/MWNT	–	–	–
1% Rh/MWNT-COOH	–	27.7	72.3
1% Rh/MWNT-COONa	12.6	39.8	47.6
9.5% Rh/MWNT-COONa	8.1	38.0	53.9
1%Rh/C*-COONa	7.3	37.4	55.3

Table 5. Main characteristics of pristine MWNTs

Internal diameter (nm)	External diameter (nm)	Real density (g·mL <sup>-1</sup> )	Pore diameter (nm)	d <sub>002</sub> (nm)	S <sub>BET</sub> (m <sup>2</sup> ·g <sup>-1</sup> )
8	17	1.95	20	0.342	180

rinsed with deionized water until the pH of the water reached 7. The resulting material was dried overnight at 383 K in a thermostatted oven and crushed to a powder by a ball-milling process for 20 min.<sup>[37]</sup> This material is named MWNT-COOH.

The preparation of the corresponding nanotube sodium carboxylate salt (MWNT-COONa) was accomplished by treatment of a suspension of 5 g of MWNT-COOH in 100 mL of toluene with 200 mg of Na<sub>2</sub>CO<sub>3</sub>·10H<sub>2</sub>O dissolved in 50 mL of H<sub>2</sub>O. This suspension was stirred for 15 min, sonicated for 2 hours at 313 K and stirred again for 15 min at room temperature. The resulting mixture was then filtered through a Büchner funnel, and the material washed with deionized water to fully remove the excess of the sodium salt. Drying overnight in a thermostatted oven at 383 K afforded MWNT-COONa. Moreover, a C\*-COONa sample was prepared for comparison purposes by the same procedure starting from a commercial activated carbon (Darco-G60, 100 mesh, S<sub>BET</sub> = 700 m<sup>2</sup>·g<sup>-1</sup>, Aldrich).

**Surface Grafting of [Rh<sub>2</sub>Cl<sub>2</sub>(CO)<sub>4</sub>] and Production of Rh/MWNTs or Rh/C\*-COONa:** 100 mg of [Rh<sub>2</sub>Cl<sub>2</sub>(CO)<sub>4</sub>] was added to a suspension of 5.29 g of the carbon support in 100 mL of toluene, stirred for 3 hours at 333 K under nitrogen and then sonicated for 2 hours at room temperature. Filtration through a Büchner funnel, washing with *n*-hexane, drying in vacuo and crushing for 20 min resulted in the production of the rhodium grafted material. Activation of the supported complex was done under a continuous flow (250 sccm) of a N<sub>2</sub>/H<sub>2</sub> gas mixture (80:20 v/v) for three hours at 573 K, then the samples were washed with water to remove the NaCl formed, dried overnight at 383 K and crushed to powder. The rhodium loading was so fixed at 1% w/w, if not otherwise specified in the text.

**Evaluation of Catalyst Activity for trans-Cinnamaldehyde Hydrogenation and Hex-1-ene Hydroformylation:** The selective hydrogenation of cinnamaldehyde was carried out at atmospheric pressure in a three-necked flask equipped with a reflux condenser and gas inlet. The mixture containing 100 mg of rhodium-supported catalyst, 2 mL of *trans*-cinnamaldehyde and 50 mL of dioxane was sonicated for 15 min at room temperature prior to each catalytic run; nitrogen gas at room temperature was bubbled through the liquid phase to purge the system, the temperature was raised to 353 K, then dihydrogen gas was let in. Each catalytic run lasted 4 h, during which time samples were taken at regular intervals for analysis.

The hydroformylation of hex-1-ene was performed in an autoclave under the following reaction conditions: 353 K, 2 MPa of CO/H<sub>2</sub> (1:1). A catalyst sample (100 mg) was dispersed in a mixture of 40 mL of toluene and 5 mL of hex-1-ene, sonicated in a Schlenk tube for 15 min and transferred under nitrogen into the autoclave, which was then pressurized and heated. At the end of the catalytic runs (24 h) the resulting mixture was cooled to room temperature, then filtered and analysed.

Analysis of the reaction products, both from hydrogenation and hydroformylation runs, was performed on a Carlo Erba HRGC 5160 gas-chromatograph equipped with a capillary column (DB-5 J&W Scientific, 30 m, i.d. 0.32 µm, film 0.25 µm); a Perkin-Elmer Q-Mass 910 GC-MS instrument (capillary column DB-1 J&W Scientific, E.I. 70 eV) was used to identify the hydrogenation or hydroformylation products and to confirm the nature of the by-products.

**Characterisation of the Materials:** TEM observations were made with a Hitachi HF2000 (200 kV) microscope equipped with a field emission gun, a cold cathode and a multiscan camera (Gatan) which allows the recording and manipulation of high-resolution images by means of Digital Micrograph software. The rhodium

particle-size distributions were determined on the basis of TEM micrographs. Additional TEM observation were performed on a Phillips CM12 (120 kV voltage) electron microscope.

Raman spectra were recorded on a T64000 Jobin-Yvon spectrometer (4 cm<sup>-1</sup> resolution) equipped with a Spectra Phisycs Argon<sup>+</sup> Laser; samples were excited at λ = 514 nm. X-ray photoelectron spectra were obtained on a VG ESCALAB MK II spectrometer. The measurements were carried out using unmonochromatized Mg-K<sub>α</sub> radiation (λ = 0.989 nm) under a mean pressure of 6 × 10<sup>-11</sup> kPa.

## Acknowledgments

Special thanks to Dr B. Richard for technical assistance and to Mr J. Y. Mevellec for his help in Raman studies. We would like to thank also Engelhard-CLAL for a generous loan of RhCl<sub>3</sub>·3H<sub>2</sub>O.

- [1] F. Rodriguez-Reinoso, *Carbon* **1998**, *36*, 159–175.
- [2] E. Auer, A. Freund, J. Pietsch, T. Tacke, *Appl. Catal. A* **1998**, *173*, 259–271.
- [3] B. Coq, J. M. Planeix, V. Brotons, *Appl. Catal. A* **1998**, *173*, 175–183.
- [4] J. E. Fischer, A. T. Johnson, *Curr. Opin. Solid State Mater. Sci.* **1999**, *4*, 28–33.
- [5] M. Menon, A. N. Andriotis, G. E. Froudakis, *Chem. Phys. Lett.* **2000**, *320*, 425–434.
- [6] K. P. de Jong, *Curr. Opin. Solid State Mater. Sci.* **1999**, *4*, 55–62.
- [7] N. M. Rodriguez, M. Kim, R. T. K. Baker, *J. Phys. Chem.* **1994**, *98*, 13108–13111.
- [8] [8a] F. Salman, C. Park, R. T. K. Baker, *Catal. Today* **1999**, *53*, 385–394. [8b] C. Park, R. T. K. Baker, *J. Phys. Chem. B* **1998**, *102*, 5168–5177.
- [9] [9a] C. Pham-Huu, N. Keller, L. J. Charbonnière, R. Ziessel, M. J. Ledoux, *Chem. Commun.* **2000**, 1871–1872. [9b] C. Pham-Huu, N. Keller, G. Erhet, L. J. Charbonnière, R. Ziessel, M. J. Ledoux, *J. Mol. Cat.* **2001**, *170*, 155–163.
- [10] R. Gao, C. D. Tan, R. T. K. Baker, *Catal. Today* **2001**, *65*, 19–29.
- [11] P. Chen, X. Wu, J. Lin, K. L. Tan, *J. Phys. Chem.* **1999**, *103*, 4559–4561.
- [12] J. M. Planeix, N. Coustel, B. Coq, V. Brotons, P. S. Kumbhar, R. Dutartre, P. Geneste, P. Bernier, P. M. Ajayan, *J. Am. Chem. Soc.* **1994**, *116*, 7935–7936.
- [13] H. Chen, J. Lin, Y. Cai, X. Wang, J. Yi, J. Wang, G. Wei, Y. Lin, D. Liao, *Appl. Surf. Sci.* **2001**, *180*, 328–335.
- [14] B. Xue, P. Chen, Q. Hong, J. Lin, K. L. Tan, *J. Mater. Chem.* **2001**, *11*, 2378–2381.
- [15] Y. Zhang, H. Zhang, G. Lin, P. Chen, Y. Yuan, K. R. Tsai, *Appl. Catal. A* **1999**, *187*, 213–234.
- [16] N. M. Rodriguez, *J. Mater. Res.* **1993**, *8*, 3233–3255.
- [17] [17a] S. Nagasawa, M. Yudasaka, K. Hirahara, T. Ichihashi, S. Iijima, *Chem. Phys. Lett.* **2000**, *328*, 374–380. [17b] A. Kuznetsova, I. Popova, J. T. Yates, Jr, M. J. Bronikowski, C. B. Huffman, J. Lin, R. E. Smalley, H. H. Hwu, J. G. Cheu, *J. Am. Chem. Soc.* **2001**, *123*, 10699–10704. [17c] T. Kyotani, S. Nakozaki, W. Xu, A. Tamita, *Carbon* **2001**, *39*, 782–785.
- [18] E. van Steen, F. F. Prinsloo, *Catal. Today* **2002**, *71*, 327–334.
- [19] V. Lordi, N. Yao, J. Wei, *Chem. Mater.* **2001**, *13*, 733–737.
- [20] T. W. Ebbesen, H. Hiura, M. E. Bisher, M. M. J. Treacy, J. L. Shreeve-Keyer, R. C. Haushalter, *Adv. Mater.* **1996**, *8*, 155–157.
- [21] Z. Liu, Z. Yuan, W. Zhou, L. Peng, Z. Xu, *Phys. Chem. Chem. Phys.* **2001**, *3*, 2518–2521.
- [22] S. Hermans, J. Sloan, D. S. Shephard, B. F. J. Johnson, M. L. H. Green, *Chem. Commun.* **2002**, 276–277.
- [23] E. S. Steigerwalt, G. A. Deluga, C. M. Lukehart, *J. Phys. Chem.* **2002**, *106*, 760–766.

- [24] B. L. Mojet, M. S. Hoogenraad, A. J. van Dillen, J. W. Geus, D. C. Koningsberger, *J. Chem. Soc., Faraday Trans.* **1997**, *3*, 4371–4375.
- [25] W. Li, C. Liang, J. Qiu, W. Zhou, H. Han, Z. Wei, G. Sun, Q. Xin, *Carbon* **2002**, *40*, 791–794.
- [26] S. Banerjee, S. S. Wong, *Nano Lett.* **2002**, *2*, 49–53.
- [27] P. Serp, R. Feurer, C. Vahlas, P. Kalck, *French Patent* 01–08511, **2001**.
- [28] Q. Yang, P. Hou, S. Bai, M. Wang, H. Cheng, *Chem. Phys. Lett.* **2001**, *345*, 18–24.
- [29] P. Serp, R. Feurer, Y. Kihn, P. Kalck, J. L. Faria, J. L. Figueiredo, *J. Phys. IV* **2002**, *12*, 24–36.
- [30] D. N. Lawson, G. Wilkinson, *J. Chem. Soc. A* **1965**, 1900–1907.
- [31] J. L. Figueiredo, M. F. R. Pereira, M. M. A. Freitas, J. J. M. Orfao, *Carbon* **1996**, *37*, 1379–1389.
- [32] U. Zielke, K. J. Huttinger, W. P. Hoffman, *Carbon* **1996**, *34*, 983–998.
- [33] A. Kazusaka, H. Suzuki, I. Toyoshima, *J. Chem. Soc., Chem. Commun.* **1983**, 150–151.
- [34] T. A. Kainulainen, M. K. Niemelä, A. O. I. Krause, *J. Mol. Cat.* **1997**, *122*, 39–49.
- [35] P. Serp, R. Feurer, C. Vahlas, P. Kalck, *French Patent* 01–13233, **2001**.
- [36] P. Serp, R. Feurer, R. Morancho, P. Kalck, *J. Catal.* **1995**, *157*, 294–300.
- [37] N. Pierard, A. Fonseca, Z. Konya, I. Willems, G. Van Tendeloo, J. B. Nagy, *Chem. Phys. Lett.* **2001**, *335*, 1–8.

Received June 19, 2002  
[I02335]